

Imaging Electrical Properties of the Human Brain using a 16-channel Transceiver Array Coil at 7T

X. Zhang¹, P-F. Van de Moortele², S. Schmitter², and B. He¹

¹Department of Biomedical Engineering, University of Minnesota, Minneapolis, Minnesota, United States, ²Center for Magnetic Resonance Research, University of Minnesota, Minneapolis, Minnesota, United States

Introduction: The electrical properties (EPs, conductivity σ and permittivity ϵ) of biological tissues can provide important information in the diagnosis of various diseases [1], and also play an important role in SAR calculation in high field (HF) MRI. Recently, the “Electrical Property Tomography (EPT)” technique has been pursued which uses electromagnetic theory to extract EP distribution *in vivo* from measured B1 maps [2-4]. In this work, we report our pilot study to reconstruct the electrical conductivity and relative permittivity distributions of the human brain, based on the previously proposed EPT algorithm [2] and using a 16-channel transceiver array coil at HF 7T MRI.

Theory: (a) Using multi-channel transceiver arrays technique, the magnitude of $\tilde{B}_{1,k}^+$ and proton density (PD) biased $\tilde{B}_{1,j}^-$ ($PD \times |\tilde{B}_{1,j}^-|$) for each channel can be measured, as well as their relative phase distributions between different channels (see Methods). It is empirically observed (from experiments and simulation data) that the sum of magnitude of all channels' $|\tilde{B}_{1,k}^+|$ profiles resembles the sum of magnitude of all $|\tilde{B}_{1,j}^-|$ profiles [5], so the relative PD distribution could be extracted by Eq. (1), and $|\tilde{B}_{1,j}^-|$ could be estimated. (b) Applying Gauss Law for magnetism, ignoring \tilde{B}_z component and according to the Principle of Reciprocity [6], we can derive Eq. (2) for each channel. Assuming the absolute phase of $\tilde{B}_{1,k}^+$ and $\tilde{B}_{1,j}^-$ for one channel unknown, with measured relative phase information, we can write a set of non-linear equations in the form of Eq. (2) which correspond to each channel, and then the absolute phase value can be retrieved by solving the equations pixel-wisely. The summation of complex $\tilde{B}_{1,k}^+$ and $\tilde{B}_{1,j}^-$ over all 16 channels will be utilized for further computation. (c) Assume isotropic EP distribution and consider the magnetic permeability inside brain tissues equal to vacuum. After combining the two central equations (Eq. (9) in [2]) into \tilde{B}_1^+ form by [6], we perform surface integration on the imaging x - y plane. Then according to the Divergence Theorem and by assuming homogeneous EP distribution within integral area S and between adjacent slices, we get Eq. (3) in which $\tilde{\epsilon}_c$ is the complex permittivity ($\tilde{\epsilon}_c = \epsilon - j\sigma/\omega$), so the EP distribution could be reconstructed. Eq. (3) could also be rearranged into the form of \tilde{B}_1^- by [6].

$$\begin{aligned} PD &\approx (\sum PD \times |\tilde{B}_{1,j}^-|) / (\sum |\tilde{B}_{1,k}^+|) \quad (1) \\ \partial \tilde{B}_1^+ / \partial x - j \partial \tilde{B}_1^+ / \partial y + \partial \tilde{B}_1^* / \partial x + j \partial \tilde{B}_1^* / \partial y &= 2(\partial \tilde{B}_x / \partial x + \partial \tilde{B}_y / \partial y) \approx 0 \quad (2) \\ -\int_S \nabla \cdot (\nabla \tilde{B}_1^+) dA &= -\int_{\partial S} \nabla \tilde{B}_1^+ \cdot \hat{n} dl = \mu_0 \omega^2 \cdot \tilde{\epsilon}_c \cdot \int_S \tilde{B}_1^+ dA \quad (3) \end{aligned}$$

Methods: Healthy volunteers who signed an IRB approved consent form were imaged with a 7T scanner (Siemens) equipped with a 16x1kW CPC RF amp (CPCTM) and an elliptical 16-channel head transceiver coil [7]. Scout images were obtained for slice positioning and B₀ field homogeneity was locally optimized (B₀ shim) within a box containing 6 contiguous axial slices chosen for the study. Subsequent 2D images were acquired at a spatial resolution of 2x2x2mm³: i) a series of 16 small flip angle GRE images with only one channel transmitting at a time while receiving on 16 channels [5,8], and ii) a long TR, short TE, GRE image used to produce a map of PD biased $\tilde{B}_{1,j}^-$, after normalization by the sinus of the excitation flip angle to remove \tilde{B}_1^+ components. A 3D map of the excitation flip angle (resolution 2x2x2mm³) was obtained with the AFI technique [9]. The 2D GRE axial head images were obtained with six averages with a total acquisition time of 15min. The 3D AFI map was obtained in 8min without average. Based on these data, $|\tilde{B}_{1,k}^+|$, PD biased $|\tilde{B}_{1,j}^-|$ and relative phase maps were calculated.

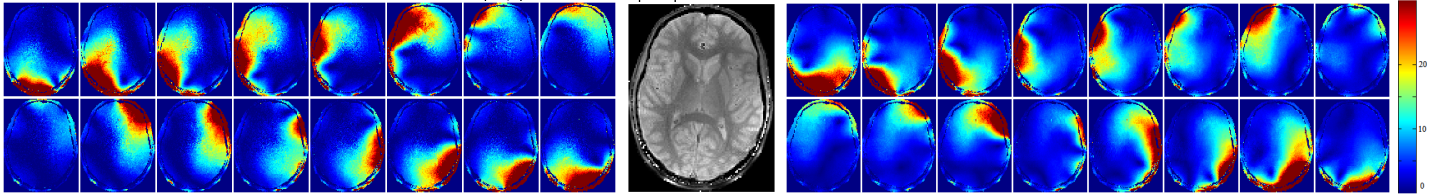


Fig. 1: (left) Measured $|\tilde{B}_{1,k}^+|$ distribution, (middle) extracted relative PD information, and (right) estimated $|\tilde{B}_{1,j}^-|$ distribution.

Results: Fig. 1 shows the measured $|\tilde{B}_{1,k}^+|$, extracted relative PD and estimated $|\tilde{B}_{1,j}^-|$ images using data on acquired slice 4, respectively. Note that the PD extraction as described in Eq. (1) enables estimated $|\tilde{B}_{1,j}^-|$ values to be evenly-scaled with $|\tilde{B}_{1,k}^+|$. Retrieved absolute phase value of $\tilde{B}_{1,k}^+$ is shown in Fig. 2. Electrical conductivity and relative permittivity distribution were calculated using Eq. (3) and are shown in Fig. 3, as well as the corresponding T1-weighted image. The CSF in the lateral ventricle can be observed in shape distinctly in both reconstructed EP images and with values of $\sigma_{CSF} = 2.01 \pm 0.45$ (2.22 in literature by 4-Cole-Cole Model [10]) and $\epsilon_{r,CSF} = 75 \pm 15$ (72). Within the selected ROI (indicated in Fig. 3 T1 image), the reconstructed EP values are $\sigma_{WM} = 0.45 \pm 0.20$ (0.41), $\epsilon_{r,WM} = 50 \pm 11$ (44), and $\sigma_{GM} = 0.72 \pm 0.33$ (0.69), $\epsilon_{r,GM} = 55 \pm 12$ (60), respectively.

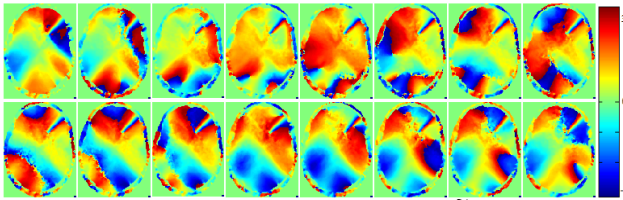


Fig. 2: Reconstructed absolute phase distribution of $\tilde{B}_{1,k}^+$ of 16 channels.

Discussion and Conclusion: $|\tilde{B}_1^-|$ mapping and absolute phase retrieval remain to be challenging issues. In this study, using multi-channel transceiver arrays, we developed a new method to reconstruct $|\tilde{B}_{1,j}^-|$ and phase of $\tilde{B}_{1,k}^+$ and $\tilde{B}_{1,j}^-$. Furthermore, we demonstrate *in-vivo* imaging of electrical conductivity and relative permittivity distribution in a human brain at 7T. Establishment of noninvasive imaging modality for EP imaging may have a significant impact in neuroscience research and clinical applications, and may also facilitate SAR computation in HF-MRI.

References: [1] Fear EC et al., IEEE TBME 2002, 49(8): 812-822. [2] Zhang XT et al., IEEE TMI 2010, 29(2): 474-481. [3] Katscher U et al., IEEE TMI 2009, 28(9): 1365-1374. [4] Voigt T et al., ISMRM 2010, 2865. [5] Van de Moortele PF et al., ISMRM 2007, 1676. [6] Hoult DI, Concepts Magn. Reson. 2000, 12(4): 173-187. [7] Adriany G et al., MRM 2008, 59: 590-597. [8] Van de Moortele PF et al., MRM 2005, 54: 1503-1518. [9] Yarnykh VL, MRM 2007, 57:192-200. [10] Gabriel C et al., PMB 1996, 41: 2251-2269. **Acknowledgment:** NIH R01EB007920, R01EB006433, R21EB006070, P41 RR008079, P30 NS057091, and WM KECK Foundation.

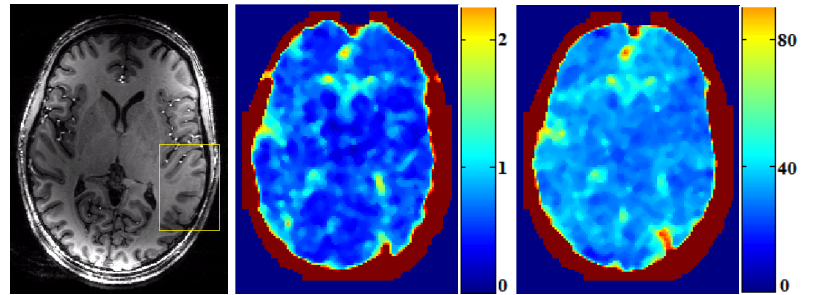


Fig. 3: (left) T1-weighted image, (middle) reconstructed σ (S/m) image, and (right) reconstructed ϵ_r image.